All-optical generation of DFT-S-OFDM superchannels using periodic sinc pulses

Arthur James Lowery, Chen Zhu, Emanuele Viterbo and Bill Corcoran

Centre for Ultrahigh bandwidth Devices for Optical Systems (CUDOS), Department of Electrical and Computer Systems Engineering, Monash University, VIC 3800, Australia
arthur.lowery@monash.edu

Abstract: Discrete-Fourier-transform spread (DFT-S) optical Orthogonal Frequency Division Multiplexed (OFDM) signals offer improved nonlinearity performance in long haul optical communications systems, and can be used to form superchannels. In this paper we propose how DFT-S-OFDM superchannels can be generated and demultiplexed using all-optical techniques, and demonstrate the feasibility using numerical simulations. We also discuss how each wavelength channel is similar to recently proposed Orthogonally Time-Division Multiplexed (OrthTDM) systems using periodic-sinc pulses from, for example, a Nyquist laser. The key difference between OrthTDM and DFT-S-OFDM is the synchronization of the symbol boundaries of every modulation tributary; because of this we show that OrthTDM cannot be formed into superchannels that can be demultiplexed without penalties, but DFT-S-OFDM can be.

©2014 Optical Society of America

References and links

1. M. Wu and Z. Qiu, "Power de-rating reduction for DFT-S-OFDM system," in *Wireless, Mobile and Multimedia Networks, 2006 IET International Conference on* (Hangzhou, China, 2006), pp. 1–4.
2. Q. Yang, Z. He, Z. Yang, S. Yu, X. Yi, and W. Shieh, "Coherent optical DFT-spread OFDM transmission using orthogonal band multiplexing," Opt. Express **20**(3), 2379–2385 (2012).
3. Y. Tang, W. Shieh, and B. S. Krongold, "DFT-spread OFDM for fiber nonlinearity mitigation," IEEE Photon. Technol. Lett. **22**(16), 1250–1252 (2010).
4. X. Chen, A. Li, G. Gao, and W. Shieh, "Experimental demonstration of improved fiber nonlinearity tolerance for unique-word DFT-spread OFDM systems," Opt. Express **19**(27), 26198–26207 (2011).
5. Y. Ma, Y. Qi, T. Yan, C. Simin, and W. Shieh, "1-Tb/s single-channel coherent optical OFDM transmission with orthogonal-band multiplexing and subwavelength bandwidth access," J. Lightwave Technol. **28**(4), 308–315 (2010).
6. G. Bosco, A. Carena, V. Curri, P. Poggiolini, and F. Forghieri, "Performance limits of Nyquist-WDM and CO-OFDM in high-speed PM-QPSK systems," IEEE Photon. Technol. Lett. **22**(15), 1129–1131 (2010).
7. R. Schmogrow, M. Winter, M. Meyer, D. Hillerkuss, S. Wolf, B. Baeuerle, A. Ludwig, B. Nebendahl, S. Ben-Ezra, J. Meyer, M. Dreschmann, M. Huebner, J. Becker, C. Koos, W. Freude, and J. Leuthold, "Real-time Nyquist pulse generation beyond 100 Gbit/s and its relation to OFDM," Opt. Express **20**(1), 317–337 (2012).
8. D. Hillerkuss, R. Schmogrow, M. Meyer, S. Wolf, M. Jordan, P. Kleinow, N. Lindenmann, P. C. Schindler, A. Melikyan, X. Yang, S. Ben-Ezra, B. Nebendahl, M. Dreschmann, J. Meyer, F. Parmigiani, P. Petropoulos, B. Resan, A. Oehler, K. Weingarten, L. Altenhain, T. Ellermeyer, M. Moeller, M. Huebner, J. Becker, C. Koos, W. Freude, and J. Leuthold, "Single-laser 32.5 Tbit/s Nyquist WDM transmission," J. Opt. Commun. Netw. **4**(10), 715–723 (2012).
9. G. Bosco, V. Curri, A. Carena, P. Poggiolini, and F. Forghieri, "On the performance of Nyquist-WDM terabit superchannels based on PM-BPSK, PM-QPSK, PM-8QAM or PM-16QAM subcarriers," J. Lightwave Technol. **29**(1), 53–61 (2011).
10. M. Nakazawa, T. Hirooka, P. Ruan, and P. Guan, "Ultrahigh-speed "orthogonal" TDM transmission with an optical Nyquist pulse train," Opt. Express **20**(2), 1129–1140 (2012).
11. M. A. Soto, M. Alem, M. Amin Shoaie, A. Vedadi, C. S. Brès, L. Thévenaz, and T. Schneider, "Optical sinc-shaped Nyquist pulses of exceptional quality," Nat. Commun. **4**, 2898 (2013).
12. M. Nakazawa, M. Yoshida, and T. Hirooka, "The Nyquist laser," Optica **1**(1), 15–22 (2014).

13. J. Zhang, J. Yu, Y. Fang, and N. Chi, "High speed all optical Nyquist signal generation and full-band coherent detection," Sci. Rep. **4**, 06156 (2014).
14. W. Shieh and C. Athaudage, "Coherent optical orthogonal frequency division multiplexing," Electron. Lett. **42**(10), 587–588 (2006).
15. O. Gaete, L. Coelho, B. Spinnler, and N. Hanik, "Pulse shaping using the discrete Fourier transform for direct detection optical systems," in *Transparent Optical Networks (ICTON), 2011 13th International Conference on*(2011), p. We.A1.2.
16. A. J. Lowery and L. B. Du, "Optical orthogonal division multiplexing for long haul optical communications: A review of the first five years," Opt. Fiber Technol. **17**(5), 421–438 (2011).
17. A. J. Lowery, "Design of arrayed-waveguide grating routers for use as optical OFDM demultiplexers," Opt. Express **18**(13), 14129–14143 (2010).
18. G. Cincotti, "Optical implementation of the Fourier transform for OFDM transmission," in *Transparent Optical Networks (ICTON), 2011 13th International Conference on*(2011), pp. 1–4.
19. M. E. Marhic, "Discrete Fourier transforms by single-mode star networks," Opt. Lett. **12**(1), 63–65 (1987).
20. J. Schröder, M. A. F. Roelens, L. B. Du, A. J. Lowery, S. Frisken, and B. J. Eggleton, "An optical FPGA: Reconfigurable simultaneous multi-output spectral pulse-shaping for linear optical processing," Opt. Express **21**(1), 690–697 (2013).
21. J. B. Schroeder, L. B. Du, M. M. Morshed, B. Eggleton, and A. J. Lowery, "Colorless flexible signal generator for elastic networks andrapid prototyping," in *Optical Fiber Communication Conference 2013*(Optical Society of America, Anaheim, California, 2013), p. JW2A.44.

1. Introduction

Discrete Fourier-Transform-Spread Orthogonal Frequency Division Multiplexing (DFT-S-OFDM) is a radio-frequency method generating waveforms with modest peak to average power ratios (PAPR), but with well-controlled spectra as expected from many-subcarrier OFDM signals [1]. Although DFT-S-OFDM was originally proposed to solve the high PAPR of mobile communications systems, which overload amplifiers and reduce power efficiency, its lower PAPR can also be an advantage in optical communications systems [2], as it has been shown to offer increased tolerance to fiber nonlinearities [3, 4]. In [2], the DFT-S-OFDM signal was generated digitally for each wavelength channel, and then the wavelengths were combined into a superchannel. A superchannel is generally arranged to maximize spectral efficiency by tightly packing wavelength channels; in the case of optical-OFDM, this can be achieved by orthogonal-band multiplexing [5]. An alternative method of forming superchannels is "Nyquist-WDM" [6]. Nyquist WDM signals modulate each data symbol onto a sinc-shaped pulse. For one wavelength channel, the pulses are arranged to overlap so the peak of one pulse aligns with the nulls of all other pulses, to enable orthogonal demultiplexing [7]. Practical sinc-pulses have near rectangular spectra, enabling neighboring wavelength channels to be closely packed without overlap, to form a Nyquist-WDM superchannel [8, 9].

In 2011 Nakazawa *et al*. proposed an "Orthogonal" Time-Division Multiplexed (OrthTDM) system using a "Nyquist pulse train" [10]. This used a Mode-Locked Laser (MLL) followed by a pulse shaper to create a pulse train mathematically equivalent to a Dirac pulse train convolved with a sinc pulse; in the frequency domain, this is a set of N equally spaced phase-locked comb lines. This pulse train was then modulated with baseband data, split into N paths, each path delayed by an integer number of bits, then recombined. This simulates N independent data channels, time division multiplexed together. Because the pulses are sinc pulses, their nulls can be arranged to coincide with the peaks of the wanted channel, to theoretically provide zero inter-channel interference between the TDM channels. These pulses can be demultiplexed using fast optical sampling in the time-domain.

Alternative sources of suitable pulse trains have been proposed by Soto *et al*. [11] who showed that a comb of phase-locked laser lines, bounded by a rectangular envelope, will produce the same waveform as summing sinc pulses separated by an integer multiple of their width – a train of overlapping sinc pulses – or, as named in their paper, *periodic sinc* (PS) pulses. They also suggested time-division multiplexing, to produce a wavelength channel that could be wavelength-multiplexed to produce a Nyquist WDM superchannel, but did not demonstrate a superchannel. Their source of the comb-lines was a continuous-wave (CW)

laser followed by two Mach-Zehnder Modulators (MZM), driven by phase-locked sine-waves. Nakazawa *et al*. have also proposed a "Nyquist Laser" with spectral shaping inside the mode-locked cavity [12], which produces similar sinc-shaped pulses. Zhang *et al.* have recently built a single wavelength OrthTDM system using comb lines generated by a CW laser with external modulator and filter, followed by a modulator then an optical OrthTDM multiplexer similar to Nakazawa's arrangement, but using a coherent receiver [13].

In this paper, we demonstrate that by modifying the transmitter in an OrthTDM system that uses a Nyquist pulse train (or, equivalently periodic sinc pulses) source, it is possible to generate a DFT-S-OFDM signal all-optically. Advantageously, this signal can be multiplexed to form a superchannel, and demultiplexed without loss of orthogonality, even the transmitted spectra from the DFT-S-OFDM channels spectrally overlap. This is in contrast to the previous OrthTDM transmitters [10, 11], which produce a signal that *cannot* be successfully demultiplexed after it has been formed into a densely-packed WDM superchannel; as it is not strictly a Nyquist-WDM channel, nor a DFT-S-OFDM channel. Thus, the Nyquist laser, if used in a suitable transmitter design, could become a useful source for optical implementations of DFT-S-OFDM (but not Nyquist WDM), with their inherent advantages of low PAPR and lower penalties due to fiber nonlinearity.

The paper is organized as follows. Section 2 reviews methods of generating trains of sinc pulses. Section 3 reviews the prior art of orthogonal time division multiplexing of modulated Nyquist pulse trains (OrthTDM), develops an expression for their spectra, and shows how they can be demultiplexed. Section 4 shows that OrthTDM channels can be formed into superchannels, but shows that demultiplexing of these superchannels is problematic. Section 5 introduces DFT-S-OFDM and how it can be generated electronically; this reveals a fundamental difference to OrthTDM that is the key to successful demultiplexing. Based on the understanding and formalisms presented in the previous sections, Section 6 discloses a novel method of generating DFT-S-OFDM all optically, provides equations for their time and frequency properties, and compares their spectra to OrthTDM. Section 7 presents a method of demultiplexing superchannels formed using DFT-S-OFDM, which provides perfect orthogonality. Section 8 discusses the findings and summarizes four different methods of creating superchannels. Section 9 draws the paper to a conclusion.

2. The generation of a train of sinc pulses

Figure 1 illustrates the three demonstrated methods of production periodic sinc or 'Nyquist' pulse. These should all provide similar system performance if their outputs are equivalent.
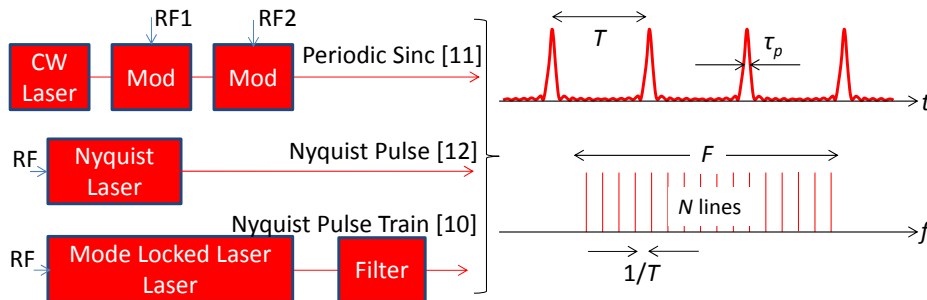
Fig. 1. Three methods of generating trains of periodic sinc or Nyquist pulses.

The optical pulses from these systems can be represented in the baseband, a convention used throughout this paper. This is equivalently the complex envelope in the complex envelope representation used in simulations. The absolute powers of the signals are ignored for simplicity.

The spectrum, $X_{PS}(f)$, of either source of 'periodic sinc' (PS) pulses is simply a number, N, of spectral lines of equal intensity, spaced by the inverse of the pulse repetition period, T. This gives sinc pulses of width $\tau_p = T/N$. For analysis, this equivalent to an infinite comb of lines (known as a Dirac comb) multiplied by a rectangular envelope of width $F = N/T$, centered so that all N lines (N even) fall within its passband, that is

$$
\begin{aligned}
X_{PS}(f) &= \operatorname{rect}_{\frac{N}{T}}(f - \frac{1}{2T}) \times \sum_{n=-\infty}^{\infty} \delta(f - n/T) \\
&= \sum_{n=-N/2+1}^{N/2} \delta(f - n/T).
\end{aligned}
\tag{1}
$$

where the rectangular function used here is:

$$
\begin{aligned}
\operatorname{rect}_{\frac{N}{T}}(f) = 1 \quad & \left[\frac{-N}{2T} < f < \frac{N}{2T} \right]; \\
0.5 \quad & \left[f = \frac{-N}{2T} \text{ or } \frac{N}{2T} \right]; \\
0 \quad & \text{otherwise.}
\end{aligned}
\tag{2}
$$

Note that the middle case of the rect function, where it returns 0.5, is not used, because of the $1/(2T)$ frequency offset in the argument of rect in Eq. (1). Mathematically the complex envelope of the optical field of the periodic sinc waveform, $x_{PS}(t)$, is the transform of the spectrum. The transform is equivalently the convolution (*) of the transform of the comb lines with the transform of the rectangular envelope of the lines, that is, the convolution of a sinc function and a Dirac pulse train. This gives:

$$
\begin{aligned}
x_{PS}(t) &= \left(\frac{N}{T} \operatorname{sin c}\left(\frac{tN}{T}\right) e^{j\frac{\pi t}{T}} \right) * \left(T.\sum_{k=-\infty}^{\infty} \delta(t - k.T) \right) \\
&= N \sum_{k=-\infty}^{\infty} \operatorname{sin c}\left(\frac{tN}{T} - k.N\right) \times e^{j\pi\left(\frac{t}{T} - k\right)} \\
&= \sum_{n=-N/2+1}^{n=N/2} e^{j\frac{2\pi n t}{T}}.
\end{aligned}
\tag{3}
$$

where the normalized sinc function is defined as:

$$
\operatorname{sin c}(x) = \frac{\sin(\pi x)}{\pi x}.
\tag{4}
$$

3. Orthogonal time division multiplexing (OrthTDM) of Nyquist pulse trains

Nakazawa *et al.* [10] demonstrated the principle of OrthTDM using a Planar-Lightwave Circuit (PLC) operating on the output of a single data modulator; obviously a real system would use separate modulators for each tributary, as illustrated in Fig. 2. This circuit should produce similar waveforms to Nakazawa's circuit in that the center of each data bit aligns with the peak of a sinc pulse, and the peaks of the sinc pulses for each tributary, m, are shifted by mT/N. The output waveform shown in Fig. 2 were simulated using VPItransmissionMaker assuming a periodic sinc source with $N = 16$ comb lines at 10-GHz apart, to create pulses of $\tau_p = 6.25$ ps FWHM, spaced at $T = 100$ ps before multiplexing. When modulated then multiplexed, this creates a 160-Gbaud pulse train. These pulses could be modulated with Quadrature Amplitude Modulation for example, to give bit rates at a multiple of the baud rate; however, to make illustration easier in the time domain, we shall use On-Off Keying (OOK)

in these examples. The intensity waveform in Fig. 2 peaks at approximately 250% higher than the peak power of one tributary the sinc functions partially overlap. Note that coupler losses are not included in this simulation.
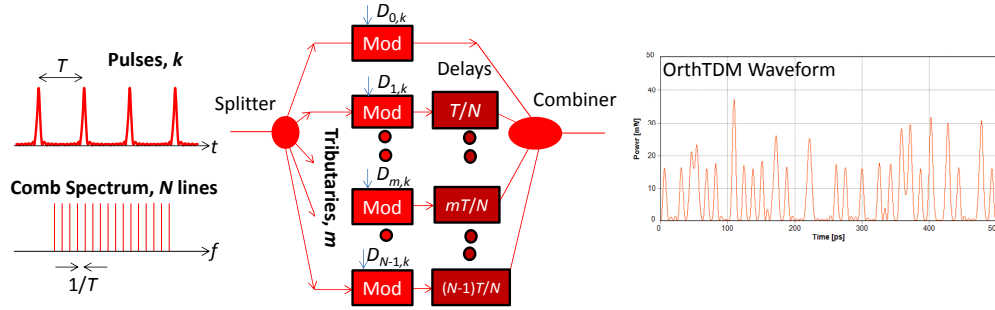
Fig. 2. Orthogonal Time Division Multiplexing (OrthTDM) of N periodic pulse trains.

The data is modulated onto each periodic-sinc pulse as illustrated in Fig. 3, to create one tributary. Non-return to zero (NRZ) OOK modulation is used, so modulation would ideally multiply each sinc pulse by either 1.0 or 0.0 over a duration T, with this interval aligned with the centers of the sinc pulses.. The tributaries are then combined, with the peak of one tributary aligned with the nulls of the sincs of all other tributaries, for orthogonality. Because there are N-1 nulls per period, there is a limit of N tributaries.
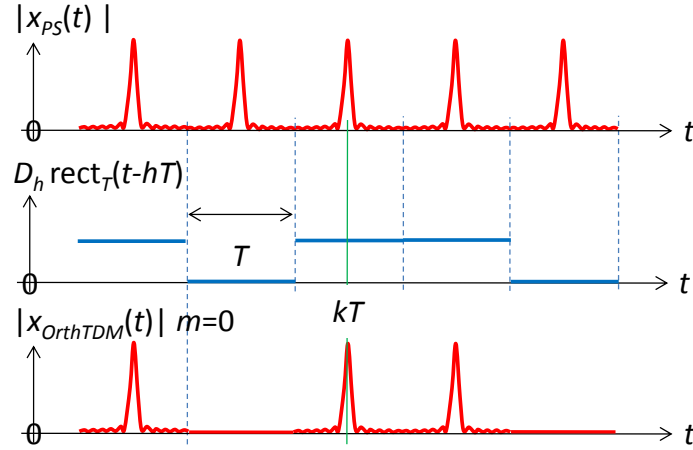
Fig. 3. Modulation of the input pulse train in one tributary ($m = 0$) of the OrthTDM multiplexer.

The baseband representation of the OrthTDM waveform for the mth tributary, ($0 \leq m < N$), is created by considering the effect of the delay (mT/N) of the PS signal that has been modulated by data $D_{m,h}$. This delay term affects both the sinc describing the PS signal, and the rect describing the modulation window of each data symbol, to produce:

$$x_{OrthTDM,m}(t) = N \sum_{k=-\infty}^{\infty} \sin c\left(\frac{tN}{T} - kN - m\right) e^{j\pi\left(\frac{t}{T} - k - \frac{m}{N}\right)} \times \sum_{h=-\infty}^{\infty} D_{m,h} \mathrm{rect}_T\left(t - hT - \frac{mT}{N}\right). \quad (5)$$

where the (time-domain) rectangular function used here is:

$$\text{rect}_T(t) = 1 \quad \left[-\frac{T}{2} < t < \frac{T}{2}\right];$$
$$0.5 \left[t = \frac{-T}{2} \text{ or } \frac{T}{2}\right]; \qquad (6)$$
$$0 \text{ otherwise.}$$

The baseband representation of the OrthTDM optical waveform after the combiner, $x_{OrthTDM}(t)$ is given by

$$x_{OrthTDM}(t) = \sum_{m=0}^{N-1} x_{OrthTDM,m}(t). \qquad (7)$$

3.1 Spectrum of the OrthTDM signal

The spectrum of the OrthTDM signal can be analyzed for one tributary as a convolution of the spectrum of the data with the spectrum of the comb lines. To simplify the analysis of the power spectrum of each tributary, the different delays of different paths can be ignored, since the time shift does not change to the power spectrum. As the random data, $D_{m,h}$ has a white spectrum, the power spectrum of each tributary is equal to the power spectrum of the windowed periodic sinc pulses:

$$\left|X_{OrthTDM,m}(f)\right|^2 = \left|FT\left\{\text{rect}_T(t) \times N \sum_{k=-\infty}^{\infty} \text{sin c}\left(\frac{tN}{T} - kN\right) e^{j\pi\left(\frac{t}{T} - k\right)}\right\}\right|^2. \qquad (8)$$

where $X_{OrthTDM,m}(f) = FT\left\{x_{OrthTDM,m}(t)\right\}$ and $FT\{\cdot\}$ denotes the Fourier transform operation. Equation (8) is equivalent to the convolution between the Fourier transform of the rectangular pulse of width T, and the Fourier transform of the periodic sinc pulses:

$$\left|X_{OrthTDM,m}(f)\right|^2 = \left|T \text{ sin c}\left(fT\right) * \sum_{n=-N/2+1}^{N/2} \delta(f - n/T)\right|^2. \qquad (9)$$

The modulation has a sinc spectrum, due to the rectangular modulation window function. Thus, the spectrum for one tributary is a summation of these sinc spectra over the number of comb lines:

$$\left|X_{OrthTDM,m}(f)\right|^2 = \left|T \sum_{n=-N/2+1}^{N/2} \text{sin c}\left(f - n/T\right)\right|^2. \qquad (10)$$

Figure 4 shows a time-averaged spectrum of the OrthTDM signal. The contributions to the OrthTDM spectrum from the sidebands of the tributaries add incoherently due to their uncorrelated data; whereas the carriers add coherently. This addition is in phase at the central frequency of the simulation, as the simulation assumes zero phase shifts in the delays at this reference frequency; random phase shifts in these delay paths will redistribute this carrier randomly to one or more frequencies of the original comb lines. Phase-shift keying, rather than OOK, as would be used in spectrally-efficient systems, removes the strong carrier frequencies, making the phase errors irrelevant. The modulation sidebands of each comb line leads to a nearly flat-top spectrum, with some peaking at the edges of the main band, producing 'shoulders', which are simply due to each comb line being modulated by the same data. The first peaks outside the main spectrum are also 17-dB below the main lobe, rather than 11-dB below in a standard OFDM spectrum. These spectral features are similar to the

spectra of the modulated sinc pulses presented by Soto *et al*. [11], which confirms that their pulses are modulated as in Fig. 3. Outside the extent of the original comb line spectrum there are a series of peaks and nulls. The nulls correspond to the alignment of the nulls of the modulation sidebands of each comb line.
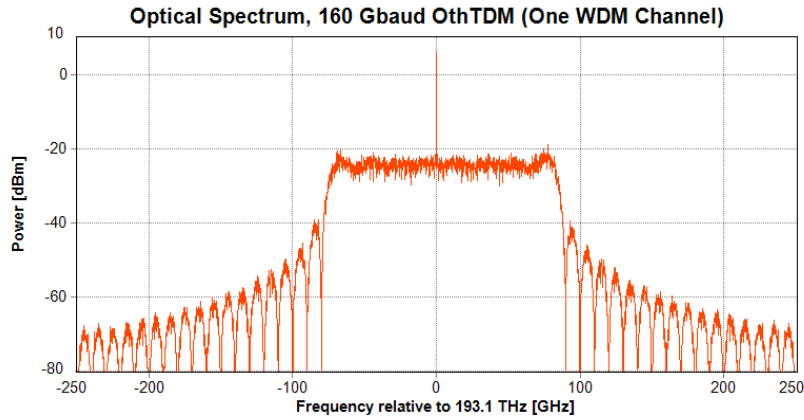
Fig. 4. Time averaged optical spectrum of the OrthTDM signal.

3.2 Demultiplexing the OrthTDM waveform

Despite the apparent complexity of the waveform in Fig. 2, it is easy to demultiplex the signal into its components by using a time-domain demultiplexer, implemented as a bank of optical samplers, assuming no unequalized distortion along the transmission path. This is because at the correct sampling time point for say, tributary (m), every other tributary has a signal with null power. Thus, at times ($kT + mT/N$), tributary m receives no interference from the other tributaries. This is easy to see from the eye diagram of the 160-Gbaud waveform shown in Fig. 5. Note that the combined signal can overshoot the valid level of the required tributary away from the correct sample point, such as in instances where there is a 1-1-0 modulation sequence.
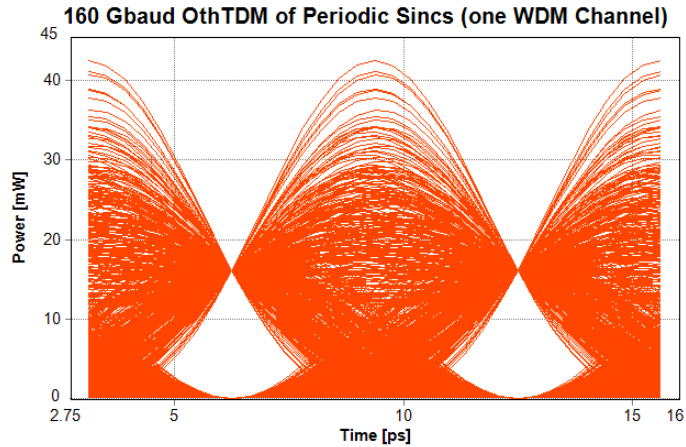
Fig. 5. Eye diagram of the OrthTDM signal showing optimum sampling points at 6.25 and 12.5 ps.

4. Multiplexing OrthTDM wavelength channels to form a WDM superchannel

The spectral efficiency gains from using Nyquist channels are only realized if they are packed into a superchannel. Because the comb lines are modulated by rectangular data pulses, the modulated spectrum has sinc-like tails, in contrast to the almost rectangular spectrum of a one wavelength channel of a Nyquist-WDM system. Despite this spectral broadening, Soto *et al.* [11] predicted that several OrthTDM channels could be wavelength multiplexed together without a guard band between them, because the nulls of the spectral tails in one OrthTDM channel (Fig. 4) would line up with the peaks of the neighboring channels. This is a similar idea to *orthogonal-band multiplexing* of Optical-OFDM [14], where the tails of one subcarrier line up with the nulls of the other modulated subcarriers, in the case of no cyclic prefix. However, there is a subtle difference that will be explored later when we attempt to demultiplex these WDM channels.

Figure 6 shows the time-averaged spectrum when three OrthTDM channels, 160-GHz apart, are multiplexed produce a guard-band-less superchannel with a nominal bandwidth of 480 GHz. Each band has a central carrier due to the DC component of the OOK modulation. Note the ripples where the edges of the bands meet, due to the overlapping spectra the wavelength channels.
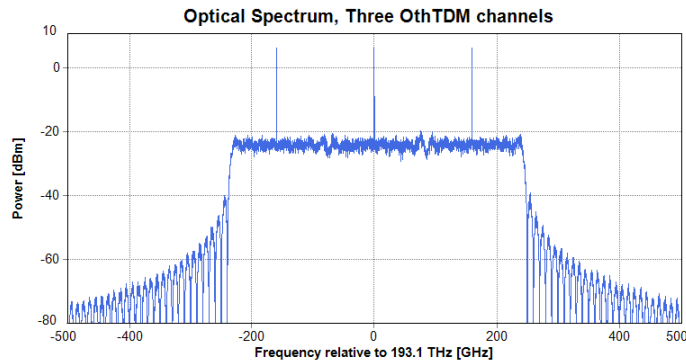
Fig. 6. Optical spectrum after combining three OrthTDM channels to form WDM.

Figure 7 shows the intensity waveform of the combined channels. The high peaks are when the fields from all channels add constructively and all three channels have high signal levels; the middle peaks are when two channels have high levels, and the lowest peaks are when one channel has a high level. The ratios of these levels are 1:4:9. The eye diagram in Fig. 8 shows these three main levels, and the zero level, at the optimum sampling time.
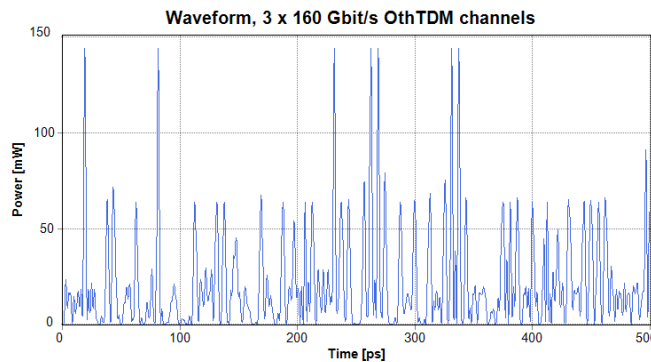
Fig. 7. Optical waveform after combining three OrthTDM channels to form a WDM superchannel.

Eye Diagram, Three OthTDM Wavelength Channels
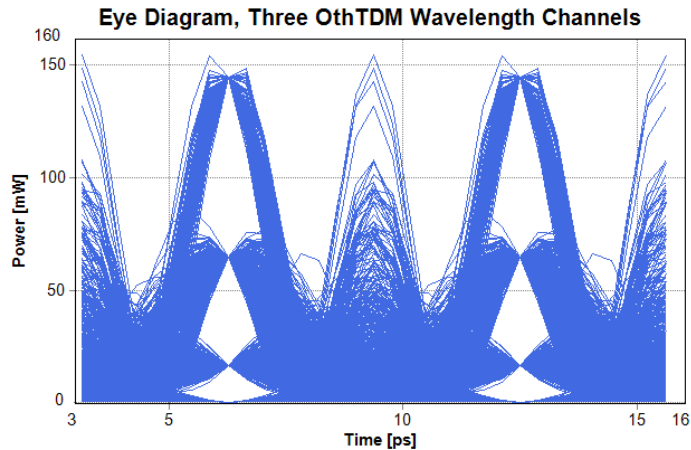
Fig. 8. Eye diagram after combining three OrthTDM channels to form a WDM superchannel.

4.1 Demultiplexing WDM OrthTDM superchannels using a band-pass filter

A simple approach to demultiplexing a channel is to use a band-pass filter. An initial approach, based on the argument that the tails of neighbouring WDM channels should not affect the required channel, would be to use a rectangular spectral shape. Figure 9 shows the eye diagram when a 160-GHz wide perfectly rectangular filter is used. When compared with the eye in Fig. 4, there is severe degradation, which could either be from the removal of the tails of the wanted channel, or from the incursion of the tails from the unwanted channels.

Eye Diagram, demultiplexed central channel from WDM
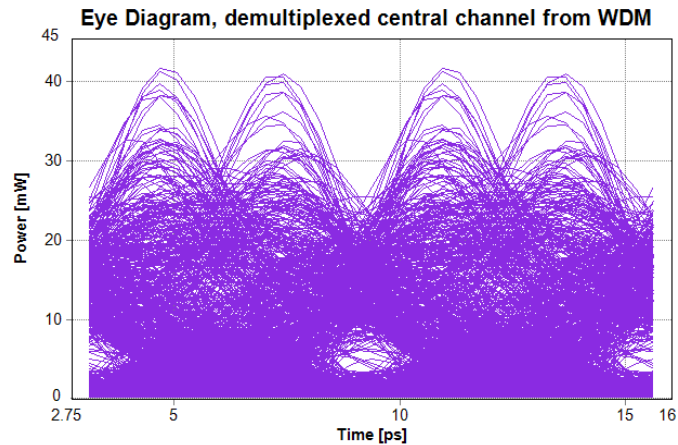
Fig. 9. Eye diagram of the central WDM channel after demultiplexing with a rectangular filter.

Figure 10 shows the same situation of filtering a channel, but with the neighbouring channels not transmitted. This has a much more open eye than shown in Fig. 9; this comparison indicates that the tails of neighboring WDM channels severely affect the wanted channel by almost completely closing the eye at the sampling point. When Fig. 10 is compared with Fig. 4 – the single channel without filtering – it is clear that the removing the spectral tails from the wanted channel causes much less eye closure than having neighbouring channels and filtering, and only of the 1-level. A conclusion from these three figures is that spectral leakage of tails from neighbouring channels' tails to within the spectrum of a wanted is important. Thus, this is not Nyquist-WDM as assumed by Soto *et al.* [11].

Eye Diagram, rectangular-filtered single OthTDM channel
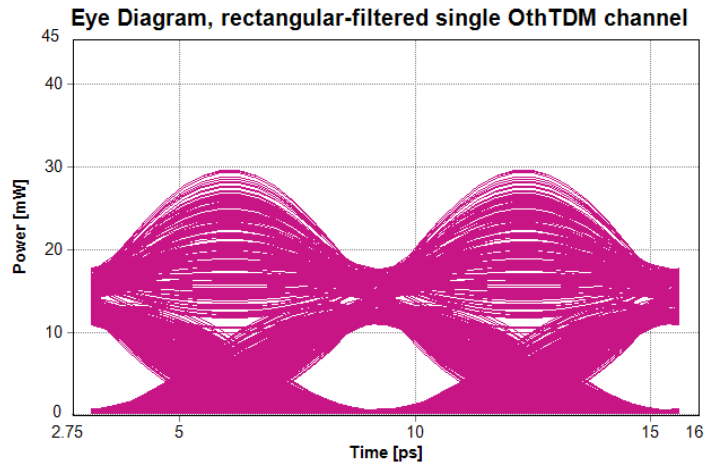
Fig. 10. Effect of a rectangular optical filter on a single transmitted OrthTDM channel.

5. Similarity of OrthTDM and DFT-S-OFDM

Optical Orthogonal Frequency Division Multiplexing (OFDM) when implemented electronically, uses an inverse Fourier transform (IFT) at the transmitter to generate a sequence of OFDM symbols [14, 15]. Each symbol contains a superposition of several subcarriers that are periodic within the symbol's duration, with the amplitude and phase of each subcarrier being set by one frequency-domain input of the IFT (*e.g.* complex data). Unfortunately, for certain phase relationships between the subcarriers (for example all are cosine-waves centered on the symbol), they will superpose to create a sinc waveform with a high peak power. The theory of Nyquist pulse generation earlier in the paper can be re-used to analyze this effect.

DFT-S-OFDM is a modification to OFDM, originally for wireless systems, with the aim of reducing the Peak to Average Power Ratio (PAPR). One or more N-point Discrete Fourier Transforms (DFT) are used to feed some of the frequency-domain coefficients of a larger IFT, based on the data input to the DFTs. Figure 11 illustrates the effect of one data input to one DFT on the output of the IFT (displayed as a waveform). The DFT produces a set of equal-amplitude outputs with linearly-increasing (or decreasing) phases that are dependent on which of its inputs is excited. The IFT uses the DFT outputs to set the phases of its subcarriers. The output waveform of the IFT (after parallel to serial conversion) will be a sinc pulse with its peak timing set by the increment rate of the phases, and thus the index of the data input [15]. Thus if several inputs of one N-point DFT are excited with non-zero data, the waveform will be a superposition of time-shifted sinc pulses, one for each data input, with the peak of one sinc pulse aligning with the (N-1) nulls of all of the other sinc pulses. If several DFTs are used, to produce a superchannel, each sinc pulse attains fine structure, due to the different subcarrier frequencies from each DFT interfering.
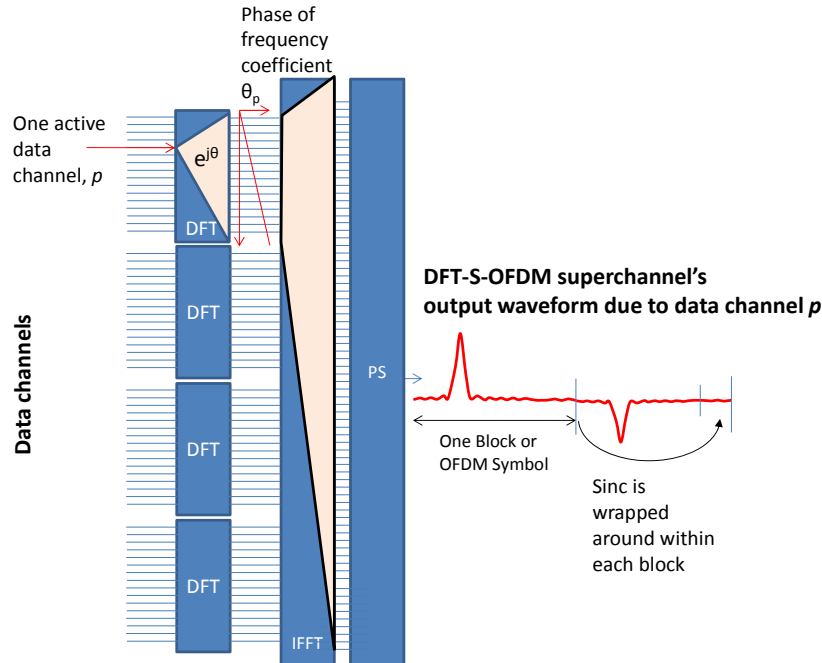
Fig. 11. DFT-S-OOFDM wavelength channel transmitter. The output waveform for a single non-zero data input is shown.

The output waveform of the IFT looks very similar to that of OrthTDM – both are time-multiplexed sinc pulses; however, there is an important difference that is critical to demultiplexing a WDM superchannel formed from DFT-S-OFDM wavelength channels. This difference is that the IFT produces sinc-pulses that are 'wrapped around' within one OFDM symbol or 'block' and do not extend beyond it. This is also illustrated in Fig. 11. Each block contains a sinc pulse that is defined by the amplitude and phase of the data signal at one input of the DFT. When the sinc pulse does not align with the center of the block, the side that would have extended beyond the block is brought into the other side of the block. This has the interesting effect that the peak of a sinc could be centered on a block boundary, for example.

The wrap-around is critical for successful demultiplexing, because it ensures that the data transitions of all of the data channels occur at the same instant, as do any transitions in the subcarriers' waveforms. In contrast, the OrthTDM scheme has many data transitions within a processing block, causing the subcarriers to be aperiodic and thus have spectral leakage into other subcarriers. This destroys orthogonality in OFDM, for example [16].

6. Creating DFT-S-OFDM waveforms with Nyquist pulses

The above comparison between OrthTDM and DFT-S-OFDM suggests a novel solution that allows demultiplexing using DFT-S-OFDM techniques. The key here is to generate sinc pulses that are 'wrapped around' within the boundaries of each OFDM symbol. This is surprisingly easy to achieve given a periodic sinc (or Nyquist) pulse source – the modulators simply have to operate on the delayed pulses, rather than the synchronized pulse sources. This is illustrated in Fig. 12.
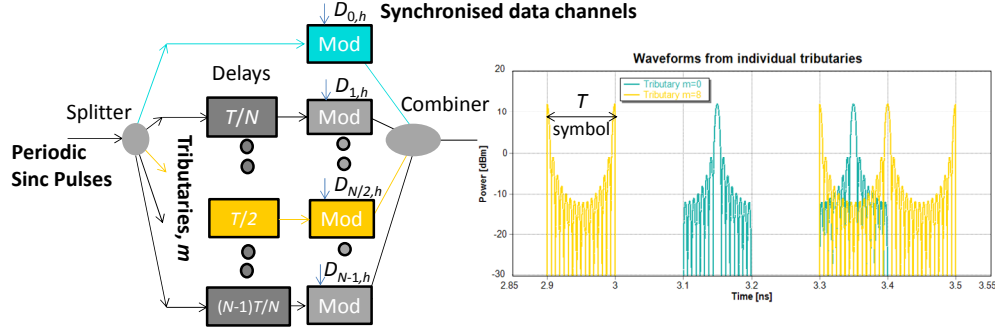
Fig. 12. One wavelength channel of a DFT-S-OFDM transmitter implemented in optics. Note how the positions of the modulators and delays have been reversed compared with Fig. 2. The data signals driving the modulators are assumed to be time-aligned. Two waveforms before the combiner are illustrated, showing how the waveform for the $N/2$ tributary wraps around within a symbol period.

The baseband representation of the DFT-S-OFDM waveform for the mth tributary, where again $m \leq N$, is created by considering the effect of the delay (mT/N) of the PS signal that has been modulated by data $D_{m,h}$. In contrast to Eq. (5), this delay term only affects the timing of the sinc describing the PS signal, and not the rect describing the modulation window, to produce:

$$x_{DFTS,m}(t) = N \sum_{k=-\infty}^{\infty} \operatorname{sinc}\left(\frac{tN}{T} - kN - m\right) \exp^{j\pi\left(\frac{t}{T} - k - \frac{m}{N}\right)} \times \sum_{h=-\infty}^{\infty} D_{m,h} \operatorname{rect}_T\left(t - hT\right). \qquad (11)$$

From Eq. (11) it is noted that the relative time shift between the periodic sinc and the modulation window cannot be ignored. The power spectrum in this case is:

$$\left|X_{DFTS,m}(f)\right|^2 = \left|FT\left\{\operatorname{rect}_T\left(t - \frac{mT}{N}\right) \times N \sum_{k=-\infty}^{\infty} \operatorname{sinc}\left(\frac{tN}{T} - kN\right) e^{j\pi\left(\frac{t}{T} - k\right)}\right\}\right|^2. \qquad (12)$$

In Eq. (12) the relative time shift term has been put into the rectangular pulse function without changing the results. Using the same argument as deriving Eq. (10), we can explain the spectrum of each tributary of the DFTS-OFDM signals as the convolution of the sinc spectrum due to the time shifted rectangular pulse and the spectrum of the periodic sinc pulses, which leads to the final expression:

$$\left|X_{DFTS,m}(f)\right|^2 = \left|T \sum_{n=-N/2+1}^{N/2} \operatorname{sinc}\left(f - n/T\right) e^{-j2\pi(f-n/T)\frac{mT}{N}}\right|^2. \qquad (13)$$

Equation (13) shows that the power spectrum becomes different for each tributary, m, in contrast to Eq. (10), where there is no relative time shift between the periodic sinc and the modulation window.

Note that Soto *et al.* [11] showed a similar arrangement of delays then modulators to Fig. 12; however, the output waveforms were as in our Fig. 3, suggesting that the data modulation was staggered between tributaries to center the data bit around the peak of each sinc pulse, as in our Fig. 2. This is confirmed by comparing their spectra with ours – their spectrum shows the same shoulders at the edge of the main lobe as our Fig. 4, whereas the data modulation scheme in Fig. 12 produces a spectrum with a very flat main lobe, as shown in Fig. 13. This flat spectrum is a result of the summation of the spectra from the different tributaries m, each of which has strong, but different, ripples, as shown in Fig. 14 (left). For comparison, the

spectra for the individual tributaries are identical if the OrthTDM scheme with delays after the modulator (Fig. 2) is used, as shown in Fig. 14 (right).

Optical Spectrum, Three OthTDM channels
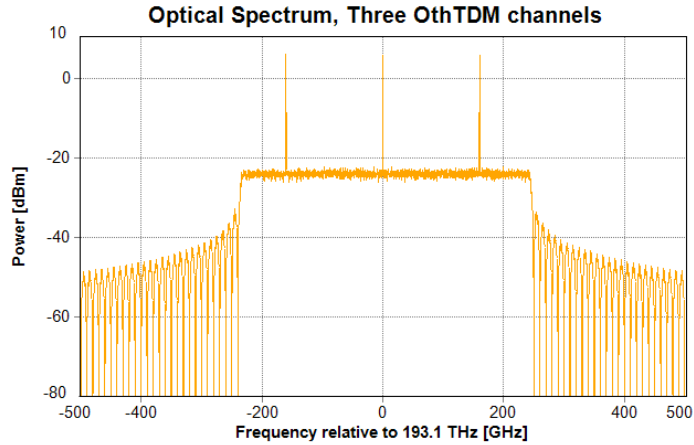
Fig. 13. Time-averaged spectrum for the 3-wavelength DFT-S-OFDM modulation system shown in Fig. 12. Note the flat top of the main lobe, which is different to that reported by Soto *et al.*
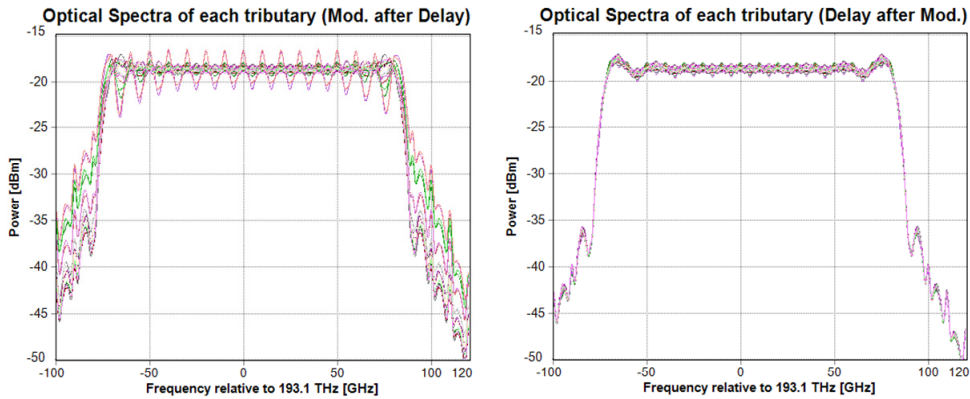
Fig. 14. Overlaid spectra for tributaries of one wavelength channel for the (left) *Modulators after Delay* (Fig. 12), and (right) *Delays after Modulators* (Fig. 2) schemes. The Modulators after Delay spectra (left) show that the relative timing of the data symbols and the peak of the sinc spectra have a dramatic effect on the spectrum of each tributary.

7. Optically demultiplexing DFT-S-OFDM superchannels

A DFT-S-OFDM receiver is simply the reverse and inverse of the transmitter; firstly a Fourier transform is used to extract each subcarrier from the received waveform. This can be achieved using a bank of filters, each with a sinc frequency response, perhaps implemented as an arrayed-waveguide grating router [17, 18], an optical Finite-impulse response filter [19], or a Waveshaper spectral processor [20]. Then the subcarrier waveforms have to be processed by an inverse (discrete) Fourier transform to extract waveforms corresponding to each data channel. This could be achieved by a second optical network. Because the outputs are only valid when the OFDM symbols overlap with the 'window' of the transform, the optical output of these networks is only valid for a short time.

In this example, three OrthTDM wavelength channels were transmitted, to form a superchannel without guard bands. The Fourier transform was implemented by a bank of 16

optical filters with sinc-responses, fed from the received signal. The bank extended over the frequency range of the center OrthTDM wavelength channel. The outputs of these filters were phase-shifted in an incremental fashion, then combined to isolate one OrthTDM tributary. The optical intensity was then detected and displayed as an eye diagram. Figure 15 shows an eye diagram when the transmitted channel that is being selected for reception is set to generate all-zeros (*i.e.*, it is nulled). There is a strong null at 100 ps, showing zero interference from other channels.
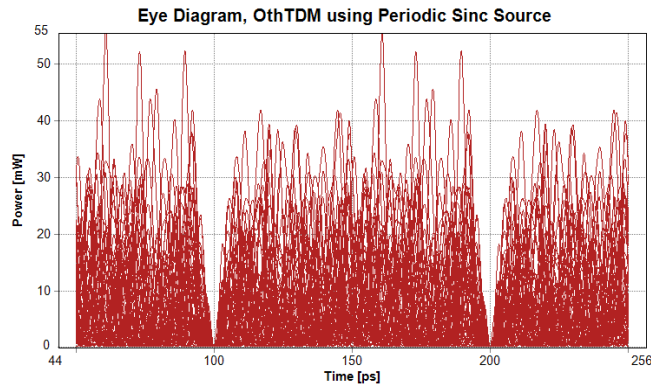
Fig. 15. Processed received signal set to receive a transmitted channel with all zeros.

Figure 16 shows an eye diagram when the transmitted channel of interest has random data (*i.e.* is not nulled). This has a very narrow eye, but a well-defined 1-level, which is only slightly broadened due to the fast transition of the sinc pulse that falls on the symbol boundary. The narrowness of the eye is due to the very large bandwidth of the received superchannel (480 GHz across the main lobe). Fast optical sampling could be used to select the waveform at this point. Note that this all-optical demultiplexing requires that chromatic dispersion and dispersion slope are compensated; alternatively, the channels can be demultiplexed and CD compensated digitally using a full band receiver [13].
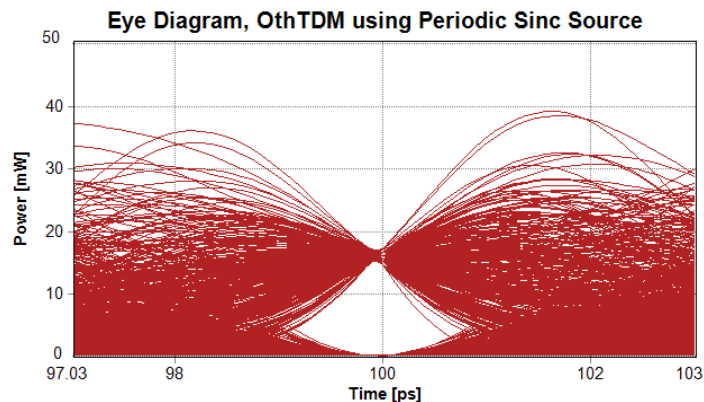
Fig. 16. Processed received signal set to receive a transmitted channel with random data (zoomed in time-axis).

We investigated the effect of the bandwidth of the modulators on the closure of the eye in Fig. 16. This showed that the tributaries with the sinc's peak close to the edge of the data modulation suffered more degradation than sincs with their peaks close to the centre of the data modulation. The signal quality is also substantially improved if the sinc having its peak split between the edges of the data bit is not transmitted. For example, a 16-GHz bandwidth

modulator (10 ps rise and fall times), gives a signal quality Q of 31 dB for the best tributary and 16 dB for the worst tributaries.

8. Discussion

The Nyquist pulse source was originally proposed to allow orthogonal time-division multiplexing [10], and performs well for OrthTDM because one channel's sinc-shaped pulses have peaks that align with the nulls of the sinc pulses of the other channels. This means it can be demultiplexed by sampling with a short sampling gate. The periodic-sinc source produces an identical pulse stream, and it has been suggested that despite its spectrum having tails that extend beyond the original rectangular spectrum, it can be wavelength division multiplexed to form a superchannel [11], because the spectral nulls of one wavelength channel align with the peaks of the neighboring channel. Unfortunately, this (time averaged) spectral feature does not tell the whole story: It does spectrally resemble an OFDM wavelength channel (apart from some shoulders on the main lobe due to the coherence of the modulation of each comb line), but it differs in that the transitions between the symbols in each subcarrier do not align in time. This means that transform-methods of separating the subcarriers have spectral leakage between the subcarrier channels, leading to a loss in orthogonality.

Fortunately, the waveform resulting from a particular data channel in OrthTDM bears a striking resemblance to the waveform from a DFT-S-OFDM channel, at least at first sight, and with a single-wavelength system. Both systems map a particular data channel onto a sinc pulse, where the identity (or index) of the channel is conveyed by the timing of the sinc pulse; however, the OrthTDM sinc pulses are always centered on the data bit period that they are modulated by so the data transitions are spread throughout the signal waveform, whereas the DFT-S-OFDM sinc pulses are wrapped-around within an OFDM symbol so that all of the transitions from one bit to another align, across all subcarriers. This means the 'block processing' using time-bounded transforms or filters can result in *orthogonal* demultiplexing. This is also true if several DFT-S-OFDM bands are multiplexed together to form a superchannel.

We have proposed a simple modification to the OrthTDM transmitter that results in signals that are identical to DFT-S-OFDM. This is to first apply incremental time delays to identical copies of the periodic-sinc pulses, then apply synchronized modulation to all tributaries. Here the periodicity of the periodic-sinc pulses plays an important role, as, once modulated, the pulses appear as though they had been created by a DFT-S-OFDM transmitter; that is, they are wrapped around to fit within a single symbol or 'block'. If several such transmitters are combined into a WDM superchannel, maintaining synchronization between the wavelength channels, then it is possible to use transform techniques to orthogonally separate the data channels. Advantageously, this signal has the properties of an optical DFT-S-OFDM superchannel, in that it should be tolerant to fiber nonlinearities. Note that previous works [11, 13] have drawn schematics with the delays before the modulators (Fig. 12), but it is clear from the spectra and the experiment that the implementation was as our Fig. 2.

Figure 17 presents these conclusions graphically, showing how CW or pulse sources can be modulated to become a wavelength channel (left and center), which can form a superchannel (right). The green-colored superchannels can be demultiplexed without a penalty, either because their spectra are discrete (such as in N-WDM) or overlap and have synchronized modulation of every subcarrier (OFDM, DFT-S-OFDM).
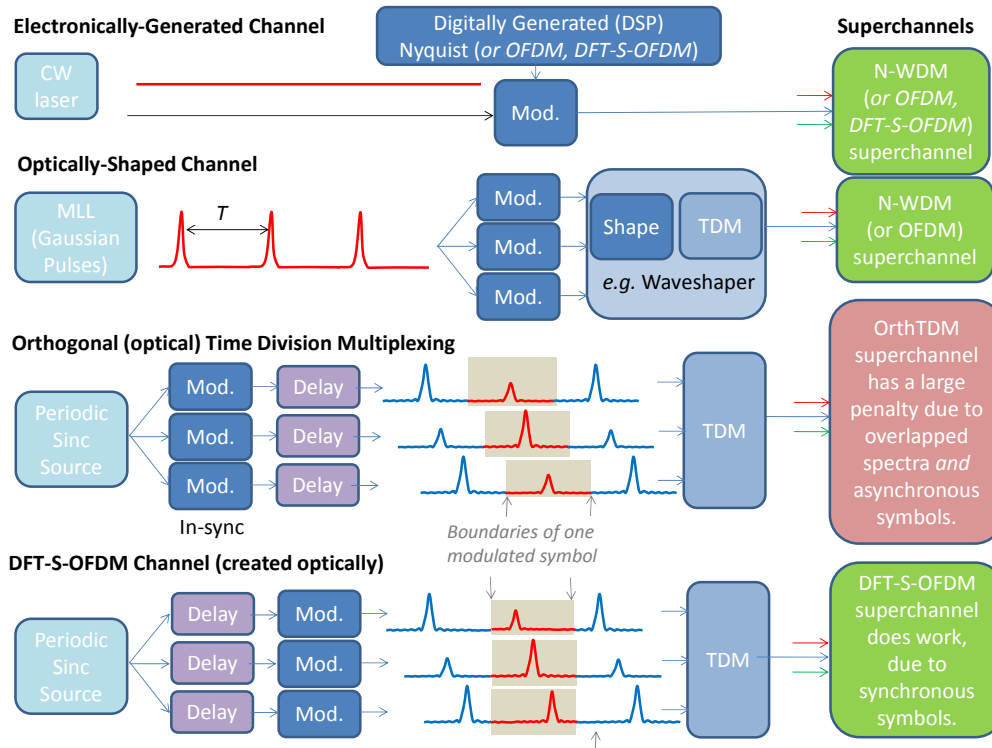
Fig. 17. One electrical (top) and three optical methods of constructing wavelength channels that can (or cannot) be used in superchannel systems. Optical pulse shaping to generate N-WDM and/or OFDM (second row) was demonstrated in [21].

9. Conclusions

In realizing parallels between OrthTDM and DFT-S-OFDM, we have been able to propose a signal format that can be orthogonally demultiplexed (albeit with high-bandwidth samplers) but also has the advantage of low PAPR and so we expect resilience to fiber nonlinearity. Interestingly, although the Nyquist pulse source provides periodic-sincs, thus at first sight seems closely related to Nyquist WDM transmission, once modulated its spectrum becomes similar to OFDM and DFT-S-OFDM in particular. It is this realization that enables transform methods to be applied to provide orthogonal demultiplexing of DFT-S-OFDM superchannels.

Acknowledgments